BIOLOGY OF REPRODUCTION (2013) **88**(1):22, 1–10
Published online before print 12 December 2012.
DOI 10.1095/biolreprod.112.105460

Profiling *Lgals9* Splice Variant Expression at the Fetal-Maternal Interface: Implications in Normal and Pathological Human Pregnancy[1]

Roy Heusschen,[4,6] Nancy Freitag,[4,7] Irene Tirado-González,[7] Gabriela Barrientos,[7] Petra Moschansky,[7] Raquel Muñoz-Fernández,[8] Ester Leno-Durán,[9] Burghard F. Klapp,[7] Victor L.J.L. Thijssen,[3,5,6] and Sandra M. Blois[2,5,7]

[6]*Departments of Radiation Oncology and Medical Oncology, Angiogenesis Laboratory, VU University Medical Center, Amsterdam, The Netherlands*
[7]*Charité Center 12 Internal Medicine and Dermatology, Reproductive Medicine Research Group, Division Psychosomatic Medicine and Psychotherapy, Medicine University of Berlin, Berlin, Germany*
[8]*Institute of Parasitology and Biomedicine "López-Neyra" Spanish National Research Council (CSIC), Armilla, Granada, Spain*
[9]*Departments of Biochemistry, Molecular Biology, and Immunology, Institute of Pathology and Regenerative Medicine, Medicine University of Granada, Granada, Spain*

ABSTRACT

Disruption of fetal-maternal tolerance mechanisms can contribute to pregnancy complications, including spontaneous abortion. Galectin-9 (LGALS9), a tandem repeat lectin associated with immune modulation, is expressed in the endometrium during the mid and late secretory phases and in decidua during human early pregnancy. However, the role of LGALS9 during pregnancy remains poorly understood. We used real-time PCR and immunohistochemical staining to analyze the expression of *Lgals9*/LGALS9 during mouse gestation as well as in human tissues obtained from normal pregnancy and spontaneous abortions. In mice, three *Lgals9* splice variants were detected, the expression of which was differentially regulated during gestation. Furthermore, decidual *Lgals9* expression was deregulated in a mouse model of spontaneous abortion, whereas placental levels did not change. We further found that the LGALS9 D5 isoform suppresses interferon gamma production by decidual natural killer cells. In human patients, six *Lgals9* splice variants were detected, and a decrease in *Lgals9 D5/10* was associated with spontaneous abortion. Altogether, these results show a differential regulation of *Lgals9* isoform expression during normal and pathological pregnancies and designate *Lgals9* as a potential marker for adverse pregnancy outcomes.

IFNG, LGALS9, normal pregnancy, splice variants, spontaneous abortion

INTRODUCTION

Galectin-9 (LGALS9) belongs to the galectin protein family, of which all members share affinity for specific β-galactoside-containing glycoproteins and glycolipids [1]. LGALS9 is a tandem-repeat galectin, consisting of two carbohydrate-binding domains (CRDs) covalently bound by a flexible linker peptide. Traditionally, the protein has been associated with regulation of the immune system during inflammation and autoimmunity [2, 3]. In addition, LGALS9 has been implicated in tumor biology [4]. The receptor for LGALS9 on immune cells is hepatitis A virus cellular receptor 2 (HAVCR2, previously known as Tim-3) [5], and several findings point toward an important role for LGALS9 in a negative-feedback loop following immune activation, preventing an excessive immune response. First, LGALS9 induces apoptosis in a variety of immune effector cells and modulates the differentiation and maturation of immune cells. For example, interferon gamma (IFNG)-producing, HAVCR2-positive T helper type 1 (TH1) cells are susceptible to LGALS9-induced apoptosis [4]. LGALS9 can also cause apoptosis in $CD8^+$ T cells [6, 7] and induce dendritic cell (DC) maturation [8]. The notion that LGALS9 is a potent immune-suppressive protein is further supported by in vivo experiments in a variety of mouse models. For instance, Wang et al. [9] demonstrated that the administration of recombinant mouse LGALS9 suppresses rejection and improves survival of allogeneic skin grafts. Besides its effects on TH1 cells, LGALS9 is also able to induce the differentiation of regulatory T cells and prevent the differentiation of proinflammatory TH17 cells from naïve T cells, suppressing collagen-induced arthritis in a dose-dependent manner [10].

Pregnancy requires well-coordinated mechanisms that modulate the maternal immune system to tolerate the fetus bearing paternal alloantigens but, at the same time, protect the mother against infections. We have previously shown that another member of the galectin family, LGALS1, is involved in the regulation of fetal-maternal tolerance [11]. Considering the immune-suppressive function of LGALS9, we hypothesized a regulatory role for LGALS9 at the fetal-maternal interface as well. This is supported by the observations that LGALS9 is expressed in human endometrial epithelial cells, with expression increasing during the mid and late secretory phases, and in decidua of early pregnancy [12–14]. We also observed LGALS9 expression in the endothelial cells of the human

[1]Supported by Charité research grant to S.M.B and by the Dutch Cancer Foundation to V.L.J.L.T. (VU2008-4101/VU2009-4358). I.T.-G. was financed by the Ministerio de Educación y Ciencia (Spain), and G.B. received a scholarship from the German Academic Exchange Service (Deutscher Akademischer Austauschdienst [DAAD]).
[2]Correspondence: E-mail: sandra.blois@charite.de
[3]Correspondence: E-mail: v.thijssen@vumc.nl
[4]These authors contributed equally to this work.
[5]These authors jointly supervised this work.

Received: 10 October 2012.
First decision: 30 October 2012.
Accepted: 5 December 2012.

eISSN: 1529-7268 http://www.biolreprod.org
ISSN: 0006-3363

placenta [14]. In addition, bovine early gestational endometrial cells, late gestational trophoblasts, and maternal epithelial and stromal cells express LGALS9 [15].

Analysis of LGALS9 expression is complicated by the observation that cells can express multiple LGALS9 isoforms [14, 16], which can exert diverging functions [17, 18]. Thus, characterization of *Lgals9* splice variant expression is important to gain insight regarding the role of this protein during pregnancy. In the present study, we set out to analyze, to our knowledge for the first time, the expression of multiple *Lgals9* splice variants during gestation, in both normal pregnancy (NP) and spontaneous abortion (SA). Furthermore, we highlight differences in the expression of *Lgals9* splice variants at the fetal-maternal interface. Our results designate the *Lgals9* splice variant profile as a potential marker for adverse pregnancy outcome as well as an important player at the fetal-maternal interface during both normal and pathological pregnancies.

MATERIALS AND METHODS

Human Tissue Collection

Spontaneous abortion samples from first-trimester pregnancies (gestation, 6–11 wk) were collected at the Gynecology Department, San Cecilio University Hospital (Granada, Spain). SA was confirmed by ultrasonography and bleeding. Specimens from elective terminations of pregnancy (gestation, 6–11 wk) were obtained from the Clínica El Sur (Malaga, Spain) and Ginegranada Clinic (Granada, Spain). Decidual-placental tissue was obtained by suction curettage; in SA, curettage was carried out within 24 h after diagnosis. None of the samples showed any evidence of necrosis or acute inflammation. All patients provided written informed consent for the collection of samples and subsequent analysis. This study was approved by the institutional review board at the University of Granada (Spain) and Charité (Berlin, Germany). Characteristics of the recruited participants are summarized in Table 1.

Animals

Mice were purchased from Janvier SAS and maintained in an animal facility with a 12L:12D photoperiod. CBA/J females were caged with DBA/2J or Balb/c males overnight and examined for a vaginal plug the next morning. The presence of a plug was designated as Gestational Day (GD) 0.5. Gravid females were killed on GDs 7.5 and 13.5 (n = 5–7 per group per day analyzed). Uteri and placentae were removed and divided into pieces for RNA isolation followed by real-time PCR, and complete implantations were frozen for immunohistochemistry. Of note, samples from GD 7.5 contained both mesometrial decidual (MD) and antimesometrial decidual (AMD) compartments, whereas samples on GD 13.5 included decidua basalis (DB) and mesometrial lymphoid aggregate of pregnancy (MLAp). Procedures that involved mice were approved by the state authority and the Medicine University of Berlin committee on Animal Use in Research and Education.

RNA Isolation and cDNA Synthesis

Total RNA was isolated using the RNeasy Protect Mini Kit (Qiagen) according to the supplier's protocol for frozen tissue. The concentration and purity of the RNA was analyzed using the BioPhotometer plus (Eppendorf AG). After DNase digestion (Invitrogen), cDNA synthesis was performed using random primers (Invitrogen) on 1 μg of RNA. Nuclease-free water was added up to a final volume of 20 μl.

TABLE 1. Characteristics of the recruited participants.

Parameter	Normal pregnancy (n = 18)[a]	Spontaneous abortion (n = 22)[b]
Age (yr)	25.3 ± 3.40	28.1 ± 4.20
Gestational age (wk)	6–11	6–11

[a] Inclusion criteria for NP group: 6–11 wk of gestation, no fertility treatment, no infection with hepatitis B/C or human immunodeficiency virus; and no signs of an imminent miscarriage, such as vaginal bleeding, low beta human chorionic gonadotropin, or missing embryonic/fetal heart rate during ultrasound screening.

[b] Exclusion criteria for the SA group: molar pregnancies, abnormal fetal karyotype, infection-induced abortion, recurrent miscarriage, and autoimmune or other systemic or local diseases.

Real-Time PCR

Real-time PCR was performed on the CFX96 Real-Time PCR Detection System (Bio-Rad) using a standard two-step amplification protocol (annealing temperature, 61°C) followed by a melting-curve analysis. For each reaction, 1.5 μl of cDNA was used in a total volume of 25 μl containing 1× SensiMix (Quantace) and 400 nmol/L of both the forward and reverse primer. Primers were designed to target specifically human or mouse *Lgals9* splice variants (Supplemental Fig. S1, available online at www.biolreprod.org, and Table 2). All primers were synthesized by Eurogentec.

LGALS9 Immunohistochemistry

After deparaffinization and rehydration, serial human and mouse paraffin-embedded tissue sections (section thickness, 4 μm) were washed in Tris-buffered saline (TBS), followed by blocking of endogenous peroxidase through incubation with 3% H_2O_2 in methanol for 30 min at room temperature. After incubation with 2% normal serum for 20 min, primary antibody against LGALS9 (1:100, sc-19292; Santa Cruz Biotechnology) was incubated overnight at 4°C. The slides were then washed and incubated with donkey anti-goat horseradish peroxidase-conjugated secondary antibody (1:200, 705-035-147; Jackson ImmunoResearch) for 1 h at room temperature. The signal was detected using the Liquid DAB+ Substrate Chromogen System (K3467; Dako) at room temperature. After washing, nuclei were counterstained with 0.1% Mayer hematoxylin followed by a standard dehydration procedure and mounting in Vitro-Clud medium (R. Langenbrinck). Negative controls with irrelevant immunoglobulin (Ig) G showed no specific immunoreactivity. LGALS9-positive cells in mouse samples were enumerated in the central and lateral regions of the MD and AMD (GD 7.5) or DB and MLAp (GD 13.5) on three or more sections per implantation site from both NP and SA groups. In addition, LGALS9-stained human samples were analyzed using ImageJ software (National Institutes of Health), and the number of positive pixels per area was measured digitally, indicating the level of expression for LGALS9 staining. The ImageJ software identifies and measures positive cells by setting a threshold. After predefining the threshold of an LGALS9-positive cell, an automatically running function was performed.

Dolichos biflorus *Agglutinin Lectin/LGALS9 Dual Staining*

Uterine tissue sections from GD 13.5 were stained following our standard protocol [11]. Briefly, slides were washed three times in TBS for 5 min, blocked with 2% normal serum for 20 min, and incubated overnight at 4°C with the primary antibody LGALS9 (1:100, sc-19292; Santa Cruz Biotechnology). Negative control was established by replacing the primary antibody with irrelevant IgG. After washing with TBS, LGALS9-stained sections were incubated for 1 h at room temperature with fluorescein isothiocyanate-conjugated secondary antibodies (1:200, 703-096-147; Jackson ImmunoResearch). Biotinylated conjugated *Dolichos biflorus* agglutinin (DBA) lectin (1:2000, L6533; Sigma-Aldrich) [19] was incubated overnight at 4°C followed by Rhodamine Avidin D, TRITC (1:200; A-2002; Vector Laboratories) for 1 h at room temperature. Nuclei in all sections were counterstained by incubation for 5 min in 4′,6-diamidino-2-phenylindole solution, followed by washing with TBS and mounting in Immu-Mount medium (Shandon). Sections were analyzed using a confocal laser-scanning microscope (cLSM 510; Carl Zeiss).

Decidual Natural Killer Cell Purification and Cell Culture

Uteri were collected, washed with sterile PBS, carefully cut into small pieces, collected in tubes containing sterile Hanks balanced salt solution (HBSS), and digested for 20 min at 37°C under slight agitation in HBSS with 200 U/ml of hyaluronidase (H3506; Sigma), 1 mg/ml of collagenase (type C-2139; Sigma), 0.2 mg/ml of DNase I (1284932; Boehringer Mannheim GmbH), and 1 mg/ml of bovine serum albumin/fraction V (A9418; Sigma). Thereafter, the isolated cells were collected in a fresh tube through a 40-μm net (Becton Dickinson) and washed with RPMI 1640-10% fetal bovine serum (FBS). The procedure was repeated twice, with sterile HBSS medium containing no cocktail of enzymes. Cells were resuspended and centrifuged at 1500 rpm for 10 min at room temperature. Trypan blue exclusion revealed that cell viability was approximately 95%. We then isolated the killer cell lectin-like receptor subfamily B member 1C (KLRB1C; previously known as NK1.1)-positive cell fraction by magnetic-activated cell sorting (MACS). For collection of cells expressing KLRB1C to use in cell culture, uterine suspensions were incubated

TABLE 2. Primers used to specifically detect *Lgals9* splice variants in mouse and human tissue.[a]

Lgals9 splice variant	Forward	Reverse
Mouse		
ALL	CTTTCTACACCCCCATTCCA	CTCGTAGCATCTGGCAAG
FL	GCAAACAGAAAACTCAGA	TCCACAGCGAAGGTTGATA
D5	ATCACCTTCCAG][ACTCAG	TCCACAGCGAAGGTTGATA
D6	GCAAACAGAAA][GCTCAAACT	TCCACAGCGAAGGTTGATA
DD10	GCAAACAGAAAACTCAGA	TTCACATATGATCCACAC][CTCG
D5/6	CTTTATCACCTTCCAG][GCTCA	TCCACAGCGAAGGTTGATA
D5/10	ATCACCTTCCAG][ACTCAG	TTCACATATGATCCACAC][CTCG
D6/10	GCAAACAGAAA][GCTCAAACT	TTCACATATGATCCACAC][CTCG
D5/6/10	CTTTATCACCTTCCAG][GCTCA	TTCACATATGATCCACAC][CTCG
Human		
ALL	CTTTCATCACCACCATTCTG	CTCTGAGCACTGGGCAGG
FL	GCAGACAAAAACCTCCCG	CCCAGAGCACAGGTTGATG
D5	ATCAGCTTCCAG][CCTCCC	CCCAGAGCACAGGTTGATG
D6	GCAGACAAAAA][ACCCAGACA	CCCAGAGCACAGGTTGATG
D10	GCAGACAAAAACCTCCCG	TTCACACAAGATCCACAC][CTCT
D5/6	CTACATCAGCTTCCAG][ACCCA	CCCAGAGCACAGGTTGATG
D5/10	ATCAGCTTCCAG][CCTCCC	TTCACACAAGATCCACAC][CTCT
D6/10	GCAGACAAAAA][ACCCAGACA	TTCACACAAGATCCACAC][CTCT
D5/6/10	CTACATCAGCTTCCAG][ACCCA	TTCACACAAGATCCACAC][CTCT

[a]][indicates the exon boundaries in case of intron/exon-spanning primers.

(30 min, 4°C) with biotinylated mouse anti-mouse KLRB1C (clone PK136; BD Biosciences) diluted 1:100 in labeling buffer (PBS supplemented with 2 mM ethylenediaminetetra-acetic acid). After washing with MACS buffer, cells were incubated (15 min, 4°C) with Streptavidin MicroBeads (130-048-101) and processed using MACS to collect KLRB1C-positive cells. Examination by fluorescence-activated cell sorting (FACS) revealed that greater than 95% of cells selected by miniMACS (Miltenyi Biotec GmbH) expressed KLRB1C. Cells were placed at a density of 2×10^5cells/well in the presence of recombinant LGALS9 deleted exon [D] 5 (50 or 100 nM; R&D Systems), lactose (10 mM; Sigma-Aldrich), interleukin 15 (IL15; 50 ng/ml; R&D Systems), or media and incubated for 48 h. Cultures were performed at 37°C in a 5% CO_2 atmosphere in RPMI 1640 supplemented with antibiotic (50 U/ml of penicillin and 50 μg/ml of streptomycin), 2 g/L of sodium bicarbonate, 2 mM L-glutamine, 1 mM pyruvate, and 10% FBS.

Cytometric Bead Array Analysis of Secreted IFNG

Supernatants from 48-h cell culture were harvested and stored at −80°C until cytokine testing was performed. IFNG was detected using the Cytometric Bead Array (CBA_ Mouse Inflammation Cytokine Kit (BD Biosciences). Briefly, 50 μl of each sample were mixed with 50 μl of mixed capture beads and 50 μl of the mouse inflammation phycoerythrin (PE) detection reagent consisting of PE-conjugated anti-mouse IFNG. The samples were incubated at room temperature for 2 h in the dark. After incubation with the PE detection reagent, the samples were washed once and resuspended in 300 μl of wash buffer provided by the manufacture. Data were acquired on the FACSCalibur (BD Biosciences) and analyzed using FCAP Array software (BD Biosciences). Standard curve was generated for IFNG using the cytokine standard provided by the kit. The range of IFNG detection was 20–5000 pg/ml.

Statistical Analysis

Real-time PCR data are shown as the mean ± SD. The Mann-Whitney rank-sum test was used to calculate statistically significant differences in mRNA expression. A level of $P < 0.05$ was considered to be statistically significant, and all calculations were performed using SPSS 12.0.1 software (SPSS, Inc.).

RESULTS

NP and SA Mouse Models Are Characterized by Distinct Decidual Lgals9 *Splice Variant Profiles*

To characterize LGALS9 during pregnancy, we analyzed the LGALS9 expression at the fetal-maternal interface in two mouse models. The mating of CBA/J female mice with Balb/c males analyzed in the present study defines NP, whereas the mating of CBA/J females with DBA/2J males is considered to be a mouse model for SA, in which the abortion rate (10%–15%) is increased when compared to NP (2%) [19, 20]. First, we compared decidual total *Lgals9* mRNA levels by real-time PCR between GD 7.5 (peri-implantation period) and GD 13.5 (placentation period completed). This showed that decidual total *Lgals9* mRNA expression increased from GD 7.5 to GD 13.5 in the NP and SA models, but this increase was only statistically significant in the NP model (Fig. 1A). We observed no statistically significant differences between the normal and pathological pregnancies at GD 7.5, although a trend was seen toward increased *Lgals9* expression in SA decidual tissues. As pregnancy progressed to GD 13.5, the *Lgals9* mRNA levels in deciduas from SA mice significantly increased compared to those observed in NP mice.

Next, we investigated total LGALS9 protein levels at the murine fetal-maternal interface on GD 7.5 and GD 13.5 using immunohistochemistry. During early gestation (GD 7.5), LGALS9 was observed in the vascular zone, both in the MD and the AMD. Interestingly, whereas LGALS9 in the MD was localized predominantly within the cell nucleus, it was restricted to the cytoplasm of cells in the AMD and vascular zone (Fig. 1B, left). The implantation sites of the SA females exhibited the same localization and pattern of LGALS9 expression (Fig. 1B, right), and the numbers of positive cells were comparable in both models (Fig. 1C). In advanced gestation (GD 13.5), we detected cytoplasmic LGALS9 expression in endothelial cells and natural killer (NK) cells in the MLAp (Fig. 1D, top). Additionally, endothelial cells of the spiral arteries and other maternal blood vessels (maternal lacunas) in the DB exhibited a pronounced cytoplasmic immunoreactivity for LGALS9 (Fig. 1D, bottom). The total number of LGALS9-expressing cells in both MLAp and DB was significantly elevated in SA compared to NP mice (Fig. 1E).

Knowing that LGALS9 can be expressed as multiple isoforms, we next analyzed the presence of *Lgals9* splice variants in the mouse uterus and decidua. Because *Lgals9* splicing in humans appears to be confined to exons 5, 6, and 10, we analyzed all potential combinations in the mouse samples (*D5, D6, D10, D5/6, D5/10, D6/10*, and *D5/6/10*) as well as the full-length (FL) variant. This revealed that the *FL,*

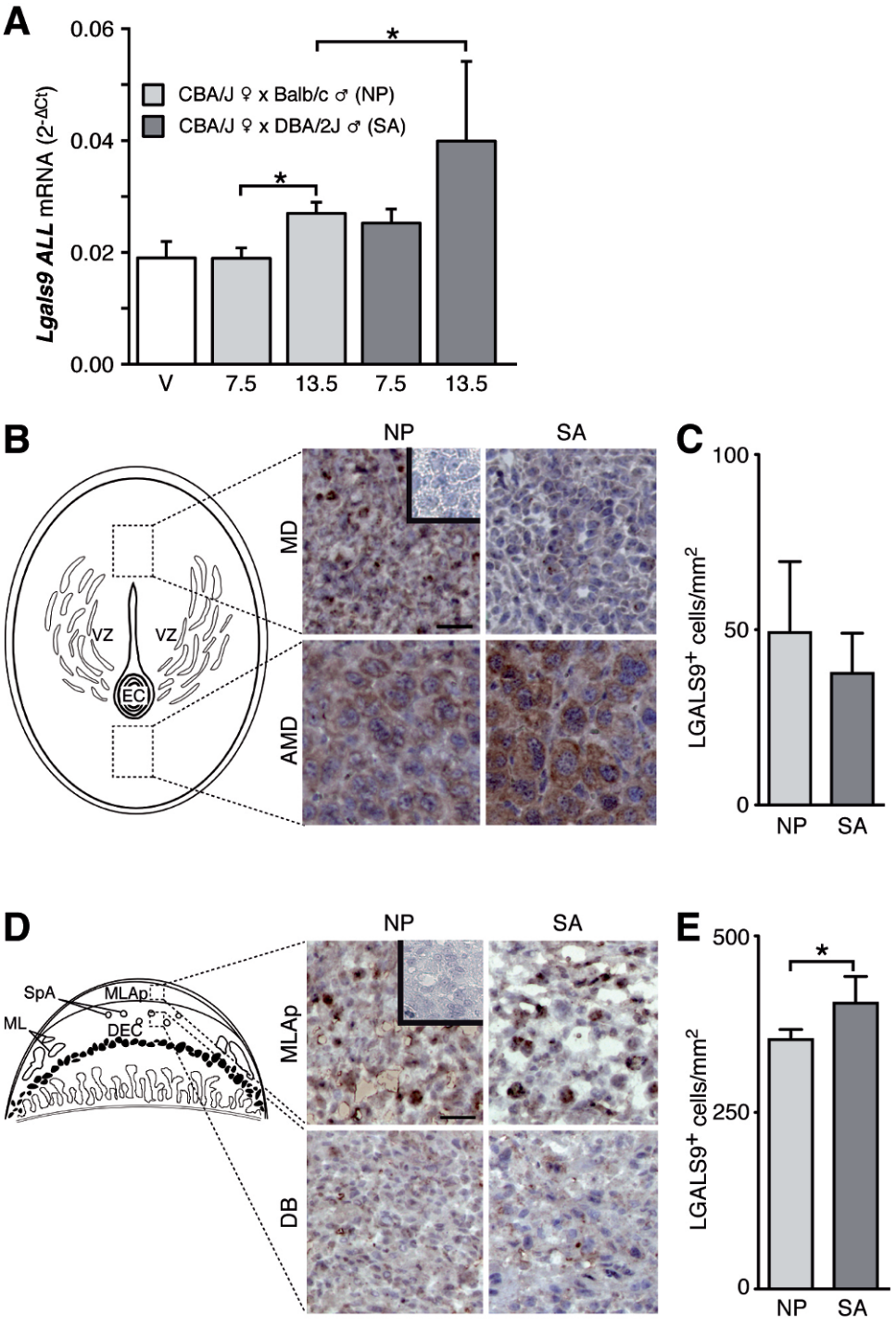

FIG. 1. LGALS9 expression in normal and pathological mouse pregnancies. **A**) Real-time PCR of *Lgals9 ALL* was performed in decidual tissue on GD 7.5 and GD 13.5 in NP (CBA/J × Balb/c; n = 5 per day analyzed) and SA (CBA/J × DBA/2J; n = 5 per day analyzed) mouse models. V, virgin female (nonpregnant uterus). Data are presented as the mean ± SD. *$P < 0.05$, Mann-Whitney rank sum. **B**) Localization of LGALS9 at the fetal-maternal interface of NP and SA mice as identified by immunohistochemistry at GD 7.5. Left: Schematic diagram of a mouse implantation site at GD 7.5. Right: Upper panels show representative stainings in the MD, lower panels in AMD. Negative control for LGALS9 staining is also shown (**inset**). EC, embryonic cavity; VZ, vascular zone. Bar = 50 μm. **C**) The number of LGALS9+ cells/mm^2 on GD 7.5 as analyzed by light microscopy using ×400 magnification. No significant differences were observed. Data are shown as mean values ± SD (n = 5–7 animals/group). **D**) Left: Schematic diagram of a mouse placenta and decidua at GD 13.5. Right: LGALS9 localization in deciduas of NP and SA mice at GD 13.5 as identified by immunohistochemistry. Upper panels show representative images of LGALS9 staining in the MLAp and lower panels in DB. Negative control for LGALS9 staining is also shown (**inset**). ML, maternal lacunas; SpA, spiral arteries. Bar = 50 μm. **E**) The number of LGALS9+ cells/mm^2 in the decidua was analyzed by light microscopy using ×400 magnification. Data are shown as mean values ± SD (n = 5–6 animals/group). *$P < 0.05$, one-way ANOVA.

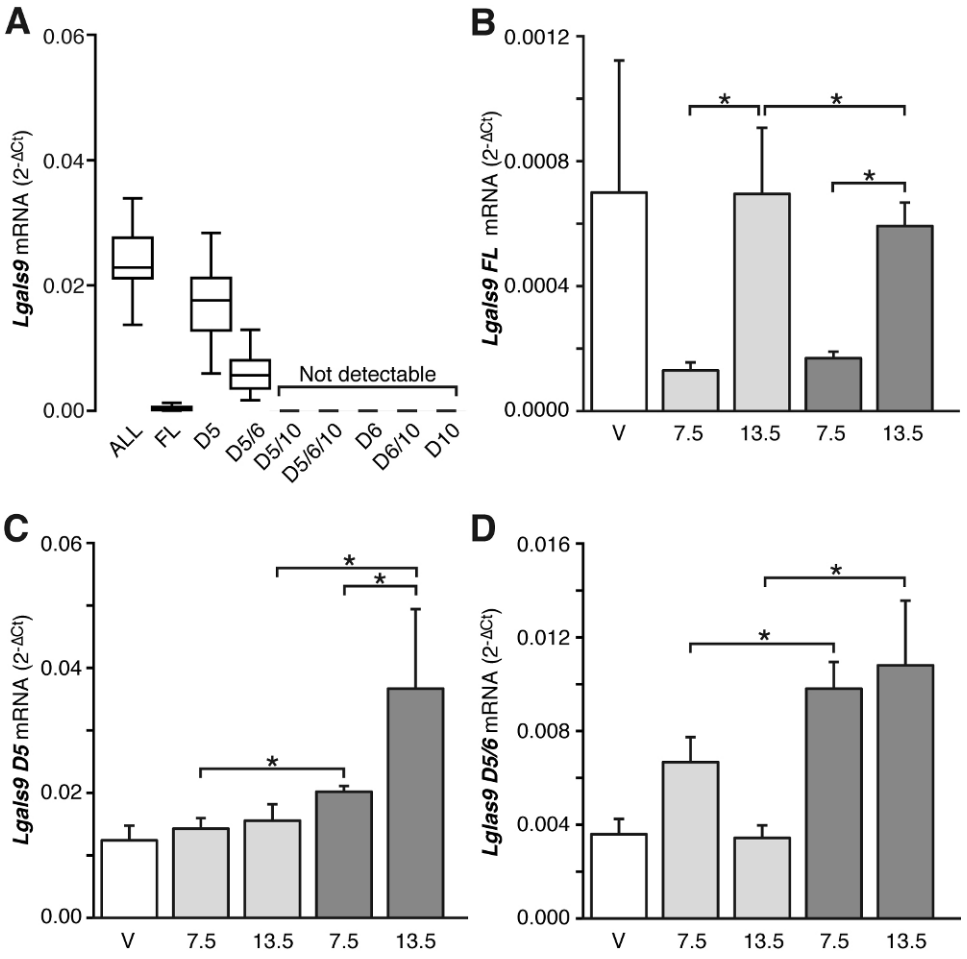

FIG. 2. Profile of *Lgals9* splice variants in normal and pathological pregnancy. **A**) *Lgals9* splice variants were determined by real-time PCR. In the murine uterus, the *FL, D5,* and *D5/6* splice variants were detected, whereas the *D6, D5/10, D6/10, D5/6/10,* and *D10* splice variants were not detectable. Real-time PCR of *Lgals9* splice variants was performed in GD 7.5 and GD 13.5 decidual tissues of NP and SA mice and in the nonpregnant uterus. Data represent mRNA expression ($2^{-\Delta Ct}$). **B**–**D**) The *FL* (**B**), *D5* (**C**), and *D5/6* (**D**) splice variants were analyzed. Data are presented as the mean ± SD (n = 5–7 animals/group). *$P < 0.05$, Mann-Whitney rank-sum test.

D5, and *D5/6* splice variants were expressed at detectable levels in the murine uterus, whereas the *D6*, *D5/10*, *D6/10*, *D5/6/10*, and *D10* splice variants could not be detected (Fig. 2A). For further analysis, we focused on the detectable variants. *Lgals9 FL* significantly increased in both NP and SA deciduas from GD 7.5 to GD 13.5 (Fig. 2B). Expression of the predominant splice variant, *Lgals9 D5*, remained unchanged during NP, whereas it was increased in SA mice from GD 7.5 to GD 13.5 (Fig. 2C). When comparing the groups to NP mice at GD 13.5, we observed that *Lgals9 D5* was increased in SA deciduas. The expression of *Lgals9 D5/6* mRNA did not change significantly in the deciduas of NP and SA mice as pregnancy progressed. In addition, *Lgals9 D5/6* expression was augmented in SA deciduas on GD 13.5 when compared to the NP model (Fig. 2D). In contrast, no differences were found in placental *Lgals9* mRNA levels of the splice variants between the NP and SA mice (Fig. 3)

LGALS9 D5 Down-Regulated the IFNG Production by Decidual NK Cells

Because the predominant splice variant *Lgals9 D5* was up-regulated in SA during the peri-implantation period (GD 7.5), we wanted to analyze the effect of the LGALS9 D5 isoform on IFNG production by NK cells. Therefore, ex vivo experiments were done to clarify whether LGALS9 D5 is involved in the regulation of IFNG production by NK cells. When decidual NK cells were treated with LGALS9 D5 (100 nM) for 48 h, IFNG secretion was down-regulated (Fig. 4A), indicating that LGALS9 D5 suppressed IFNG production by NK cells. Furthermore, we found that LGALS9 D5 suppressed IFNG secretion in a dose dependent manner (Fig. 4A). Such LGALS9 D5-mediated suppression was significantly inhibited by lactose, indicating that LGALS9 D5-mediated suppression was carbohydrate-dependent (Fig. 4A). Knowing that IFNG production by NK cells is important for maturation of the maternal vasculature and remodeling of the spiral arteries, we next evaluated the expression of LGALS9 on NK cells later during gestation (GD 13.5) in the NP and SA models. As shown in Figure 4B, a greater proportion of the NK cells (DBA lectin-positive cells) in the MLAp and DB expressed LGALS9 in the SA model compared with NP tissues.

Lgals9 D5/10 *Expression Is Decreased During Human SA*

To assess LGALS9 expression during human pregnancies, first we analyzed *Lgals9* levels of freshly isolated first-trimester samples from healthy pregnant women undergoing elective termination of pregnancy and patients with SA by real-time PCR. These samples contained both decidual and placental

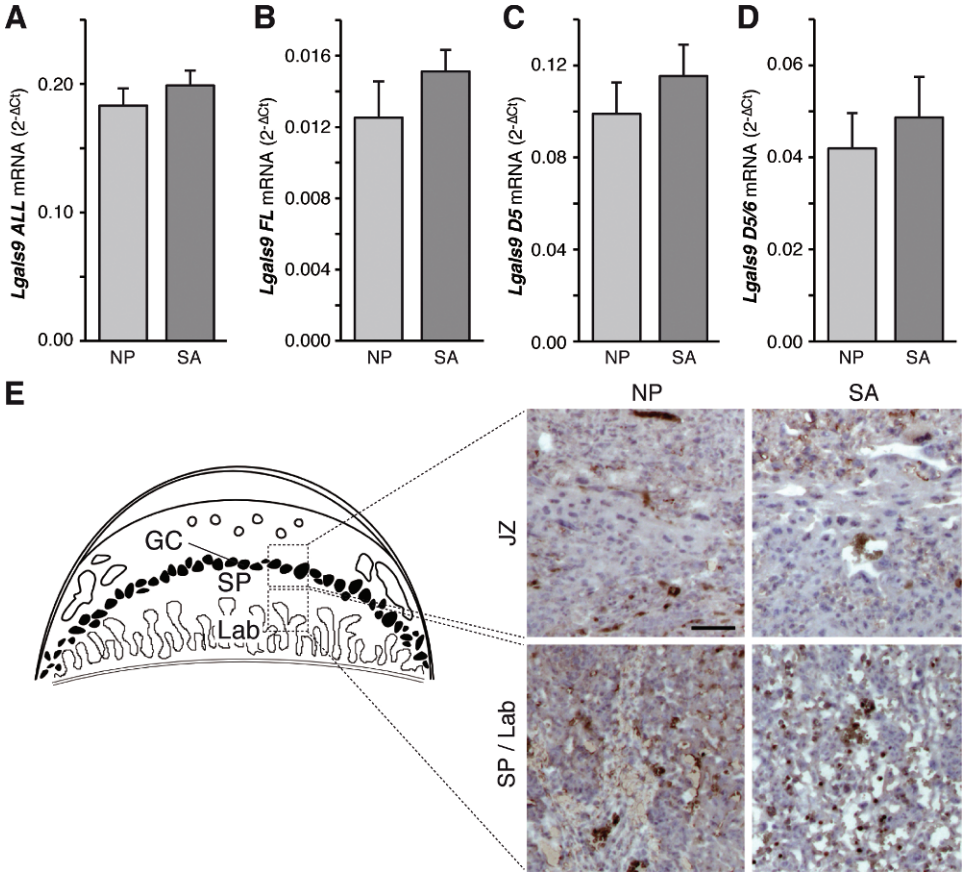

FIG. 3. Profile of *Lgals9* splice variants in placenta tissues. **A**) The total *Lgals9* level in NP and SA placentas was determined by real-time PCR at GD 13.5. The levels did not differ between the groups. **B**–**D**) The FL (**B**), D5 (**C**), and D5/6 (**D**) splice variant analyses did not show any differences between NP and SA placentas. Data represent the mRNA expression ($2^{-\Delta Ct}$), are presented as the mean ± SD (n = 5–7 animals/group), and were analyzed by Mann-Whitney rank-sum test. **E**) Immunohistochemistry was used to identify LGALS9 expressing cells within the placenta at GD 13.5. Left: Schematic diagram of murine placenta and decidua at GD 13.5. Right: The upper panels show representative images of the junction zone (JZ). The lower panels represent images of the labyrinth (Lab) compartments of the placenta. Bar = 125 μm.

compartments. Total *Lgals9 ALL* expression levels in SA tissues were similar to NP tissues (Fig. 5A). Next, we assessed LGALS9 protein expression at the fetal-maternal interface by immunohistochemistry. Decidual cells showed a strong LGALS9 expression in the cytoplasm and nucleus during NP (Fig. 5B, top left). Interestingly, the LGALS9 expression in the placental compartment, comprising stromal and cytotrophoblast cells (CTBs), was lower than in the decidua (Fig. 5B, bottom left). The protein was mostly localized to the cytoplasm of stromal cells, although some cells showed an additional nuclear staining. LGALS9 expression in CTBs was cytoplasmic, whereas the signal was absent from syncytiotrophoblasts. When comparing NP deciduas to SA deciduas, we did not observe any differences (Fig. 5, B and C). Comparable to NP placentas, the CTBs of SA placentas samples expressed LGALS9 in their cytoplasm. The localization of LGALS9 protein did not differ between both groups, but LGALS9 expression was significantly reduced in the stroma of SA placentas compared to NP placentas (Fig. 5, B and C).

To characterize the expression of *Lgals9* splice variants in normal and SA during early gestation, we analyzed the *FL, D5, D5/6, D5/10, D5/6/10,* and *D6 Lgals9* splice variants, with *FL* and *D5* being the predominant splice variants. When comparing *Lgals9* splice variant levels in NP and SA samples, we observed that *Lgals9 D5/10* was the only splice variant with significantly decreased expression in the SA group (Fig. 5D).

DISCUSSION

During pregnancy, a fine regulation of the maternal immune system induces tolerance of paternally derived antigens carried by the embryo. Nevertheless, a competitive immune system is able to protect the mother from infections. As a first step in exploring the role played by LGALS9 in this process, we characterized the expression of LGALS9 in mice and humans during NP and compared this with the expression during pathological pregnancy (i.e., SA). Because human studies during the first trimester are limited to elective interruptions and SA, we took advantage of mouse models that represent normal and pathological pregnancies. Balb/c-mated CBA/J female mice undergo normal gestations, whereas mating with DBA/2J males constitutes a mouse model for SA, in which the abortion rate (10%–15%) is increased when compared to NP (2%) [20]. Using real-time PCR, we showed a gestation-related increase of *Lgals9 ALL* in the decidua of NP mice, suggesting that *Lgals9* accompanies the course of a successful pregnancy. In this context, a shift from TH1 to TH2 cytokines occurs at the fetal-maternal interface soon after implantation (GD 5.5), which helps in the maintenance of pregnancy [21–23]. Interestingly, LGALS9 is able to limit TH1 immunity, activate tolerogenic DCs, and induce immune-regulatory mechanisms [5, 8–10], which can explain the increase of LGALS9 during the course of NP. However, we did not observe the up-regulation of *Lgals9 ALL* in the SA mouse model (CBA/J ×

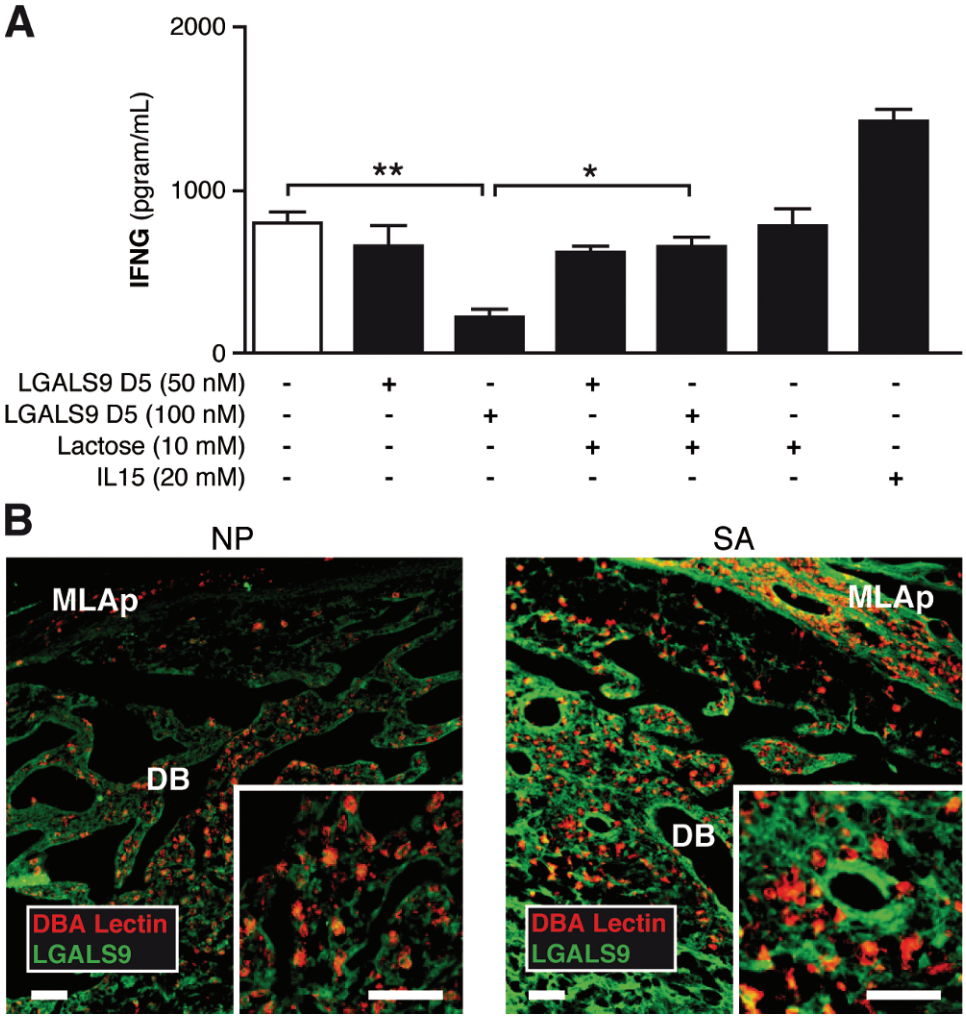

FIG. 4. Effect of LGALS9 D5 on IFNG production by decidual NK cells. **A**) LGALS9 D5 suppressed IFNG production by NK cells in a dose-dependent manner (**$P < 0.01$, ANOVA followed by Turkey test). Further, suppression of IFNG production by LGALS9 D5 (100 nM) was inhibited by lactose (10 mM, *$P < 0.05$). Data are presented as the mean ± SEM from triplicates of two independent experiments. **B**) Colocalization of LGALS9/DBA lectin was assessed on sections from GD 13.5 of NP (n = 5) and SA (n = 5) by immunofluorescence. LGALS9/DBA lectin dual staining in the DB at higher magnification (×20) is also shown (**insets**). Bar = 100 μm.

DBA/2J) from GD 7.5 to GD 13.5, confirming that a less defined TH1 and TH2 milieu characterizes this model. For instance, paternal antigens in the CBA/J × DBA/2J mouse model fail to induce the switch to TH2 cytokines after implantation [20], and as a consequence, an increase of embryo death is observed in this mating combination [24]. Thus, the notion that LGALS9 could participate in the limitation of TH1 cytokines [5] during the shift to a TH2 milieu is further supported by the impaired decidual *Lgals9* response in SA implantations.

Our results showed similar trends of *Lgals9* placental expression between the NP and SA models. Although healthy embryo-placenta units coexist with resorption sites (necrotic and hemorrhagic tissue derived from a nonhealthy placenta-embryo unit) on GD 13.5, we only included healthy implantation sites in the present study. Taking this into consideration, our data suggest that *Lgals9* expression is similar in healthy placenta units from both mouse models. However, we cannot exclude the possibility that at the beginning of the abortion process (around GD 8.5 to GD 10.5), *Lgals9* expression could be dysregulated, because *Lgals9* expression on decidual tissue is sensitive to the number of healthy embryos carried. In addition, *Lgals9* mRNA levels in the placenta are higher than in the decidua, suggesting that *Lgals9* could be important for placental development.

When studying *Lgals9* expression, it is important to note the several splice variants described to date, which differ in the inclusion of exons 5, 6, and 10 in the mature mRNA transcript. These splice variants can have diverging functions. For example, *Lgals9 FL* is a more potent eosinophil chemoattractant compared to *Lgals9 D5* [17] and is more susceptible to thrombin cleavage [25]. In addition, ectopic expression of *Lgals9 FL* decreases E-selectin expression in LoVo colon carcinoma cells, whereas *Lgals9 D5* and *Lgals9 D5/6* increase the expression of E-selectin [18]. Alternative *Lgals9* splicing is also relevant in the context of immune system modulation, because the linker length, encoded by exons 5 and 6, has been shown to influence the apoptotic effect of LGALS9 on T cells [26] and the N- and C-terminal CRDs contribute differentially to this process [27]. At the murine fetal-maternal interface, we detected the expression of *Lgals9 FL*, *Lgals9 D5*, and *Lgals9 D5/6*, with *Lgals9 D5* being the predominant splice variant. The relative amounts of each splice variant are consistent with those found in most other tissues [16]. In line with this, *Lgals9 D5* levels in the different mouse models closely resemble those we observed when assessing overall *Lgals9* levels. Of interest,

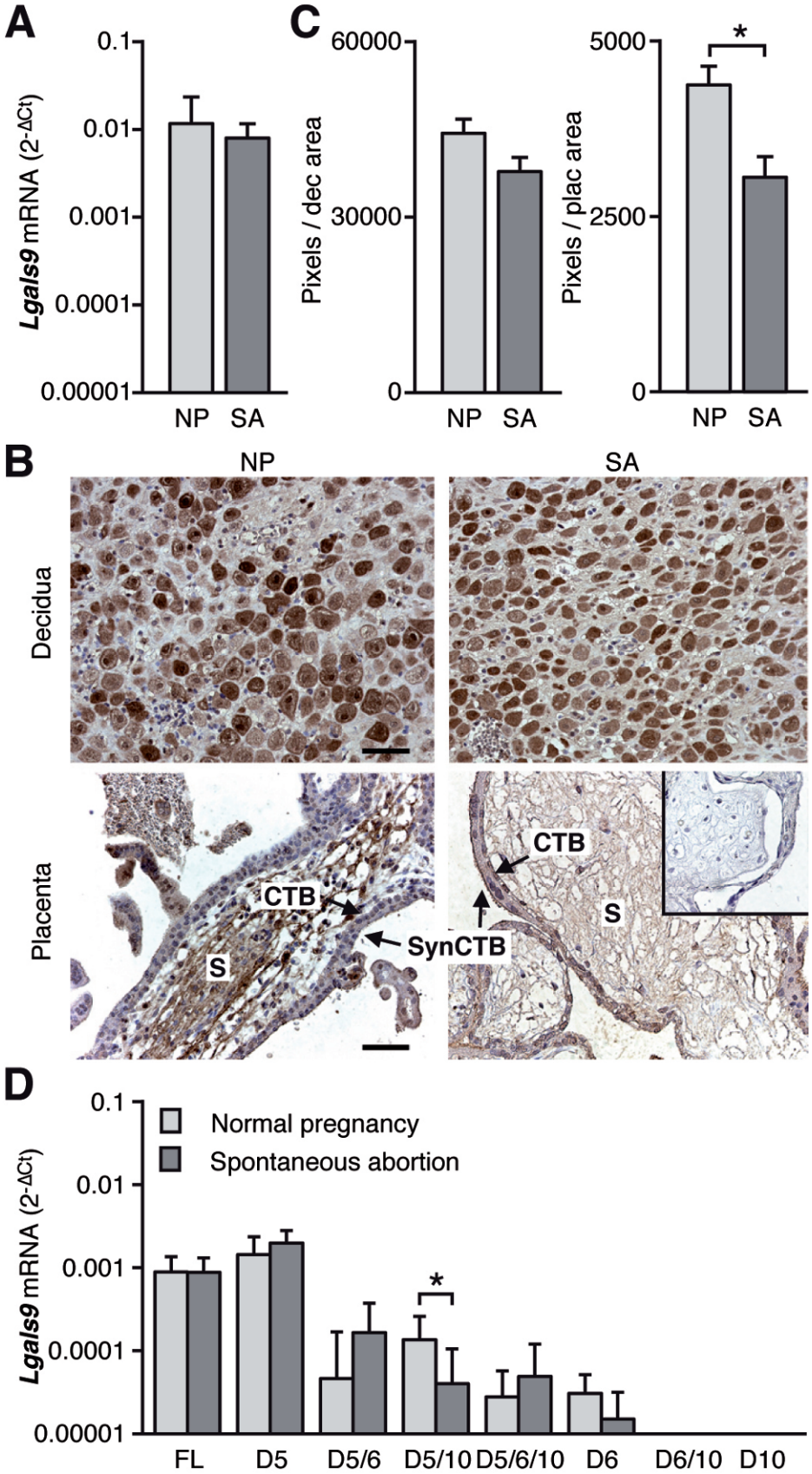

FIG. 5. *Lgals9* splice variants profile during human pregnancy. **A**) The total *Lgals9 ALL* levels did not differ between patients with NP and patients with SA. Fresh first-trimester samples (n = 18, decidua + placenta) from patients with NP and patients with SA (n = 22) were isolated, and *Lgals9* levels were measured by real-time PCR. **B**) Localization of LGALS9 was assessed in first-trimester deciduas of patients with NP (n = 18) and patients with SA (n = 22) by immunohistochemistry. Negative control for LGALS9 staining is also shown (**inset**). S, stroma; SynCTB, syncytiotrophoblasts. Bar = 100 μm. **C**) Quantification of LGALS9 staining using Image J. Graphics represent pixels/standardized area in the decidua or placenta. **D**) Messenger RNA expression levels of *Lgals9* splice variants. The difference between the NP and SA samples was significant for the *D5/10* splice variant. Data are shown as the mean ± SD. *$P < 0.05$, Mann-Whitney rank-sum test.

the increase from GD 7.5 to GD 13.5 in overall *Lgals9* levels during NP seem to result mainly from an increase of *Lgals9 FL*, because a large increase in expression of this splice variant is found, contrary to the expression of *Lgals9 D5*. Conversely, *Lgals9* D5/6 levels actually appear to decrease in NP from GD 7.5 to GD 13.5, further supporting the relevance of assessing the expression of individual *Lgals9* splice variants. Unfortunately, no antibodies are available at this time to distinguish between these variants; developing such a tool would be of great value in studying the actual functional contribution of each *Lgals9* splice variant during pregnancy.

Localization of overall LGALS9 protein at GD 7.5 was found at both the MD and AMD. Of note, in the MD, LGALS9 is localized predominantly in the nucleus, whereas in the AMD, it is localized in the cytoplasm and on the cell surface, suggesting a differential role of this lectin during early gestation. For instance, during decidualization, stromal cells differentiate into decidual cells, but only stromal cells from the AMD undergo endoreduplication and become polyploid giant cells to increase their biosynthetic capacity and thus support embryonic growth [28]. The cytoplasmic localization of LGALS9 in stromal cells from the AMD could be important for cell differentiation, because LGALS9 was reported to influence immune cell differentiation [29]. In addition, the role of this lectin in reducing cell adhesion by preventing cell binding to ligands on the vascular endothelium and extracellular matrix [30–32] could also be relevant for the AMD, in which deposition of collagen decreases less rapidly than in the MD pole during NP, preventing trophoblast invasion and migration [33].

We previously reported that the expression of LGALS9 in human umbilical vein endothelial cells is decreased, whereas the membrane-bound portion of LGALS9 is increased, upon cell activation [14]. These findings suggest that the LGALS9 level may influence stromal cell differentiation and vascular processes in the MD. Indeed, LGALS9 expression was mainly found in the granules of NK cells within the MD pole, implying that this lectin may influence their functions during pregnancy. In the present study, we provided evidence for the role of LGALS9 D5 in suppressing IFNG secretion by NK cells. Because IFNG-producing NK cells are crucial for decidual arterial remodeling into spiral arteries [34], it is tempting to speculate that LGALS9/HAVCR2 signaling could be involved in these processes. During midgestation, the maternal spiral arteries expand to increase blood flow to the placental bed [35], and mature NK cells facilitate dilation of spiral arteries [36]. Our results showed that the number of LGALS9-expressing NK cells is increased in the SA compared to the NP model, suggesting that accumulation of mature NK cells in the MLAp could be a compensatory mechanism triggered in SA to sustain placental function. Indeed, DBA/2J-mated CBA/J females showed some features of preeclampsia, in which complement activation increased tissue factor expression, causing dysregulation of angiogenic factors [37].

Finally, we profiled *Lgals9* splice variant expression in first-trimester (gestation, 6–11 wk) human samples. We did not observe any significant changes in expression of the most dominant splice variants when comparing NP to SA samples, which could be due to the fact that placental and decidual compartments were analyzed together instead of separately, as was done with the mouse samples. Whether *Lgals9* levels change significantly in the decidua and placenta during human pregnancy remains to be determined. However, we did observe a significant decrease of *Lgals9 D5/10* mRNA in samples from patients with SA. Like *Lgals9 D5/6/10* and *Lgals9 D6*, *Lgals9 D5/10* was not detected in mouse samples. In fact, *Lgals9* splice variants lacking exon 10 might be human specific [38]. At this time, no studies, to our knowledge, have reported on the functional role of *Lgals9* splice variants lacking exon 10, although initial results show these splice variants are not secreted and, presumably, act solely intracellularly [38]. Thus, it is tempting to speculate *Lgals9 D5/10* may play an important role in ensuring successful pregnancy, because a decrease of *Lgals9 D5/10* was associated with SA.

Previous studies reported on the expression of LGALS9 during the window of implantation and in normal human early decidua [12, 13]. In the present study, we provided splice variant-specific profiling at the fetal-maternal interface in both murine and human samples of NP and SA. The relevance of detecting specific *Lgals9* splice variants is supported by the diverging expression patterns and changes in expression we observed. Moreover, we showed that expression of *Lgals9* splice variants changes significantly in the decidua of the SA model compared to the NP model, providing, to our knowledge, the first line of evidence linking this disorder to dysregulated *Lgals9* expression. As such, it would be interesting to analyze the dynamics of *Lgals9* expression at the fetal-maternal interface and determine whether it could, indeed, function as a diagnostic marker for fetal loss in larger patient groups.

ACKNOWLEDGMENT

We are grateful to Evi Hagen and Petra Bußе for their technical assistance. Author contributions: V.L.J.L.T. and S.M.B. designed the research; R.H., N.F., I.T.-G., G.B., V.L.J.L.T., and S.M.B. performed the research; R.H., N.F., I.T.-G., N.F., V.L.J.L.T., and S.M.B. analyzed the data; P.M. assisted with the research; R.M.-F., E.L.-D., and B.F.K. contributed essential reagents; V.L.J.L.T., S.M.B, N.F., and R.H. wrote the manuscript.

REFERENCES

1. Wada J, Kanwar YS. Identification and characterization of galectin-9, a novel beta-galactoside-binding mammalian lectin. J Biol Chem 1997; 272: 6078–6086.
2. Rabinovich GA, Toscano MA. Turning 'sweet' on immunity: galectin-glycan interactions in immune tolerance and inflammation. Nat Rev Immunol 2009; 9:338–352.
3. Wiersma VR, de Bruyn M, Helfrich W, Bremer E. Therapeutic potential of galectin-9 in human disease. Med Res Rev 2013; (in press). Published online ahead of print 26 July 2011; DOI 10.1002/med.20249.
4. Liu FT, Rabinovich GA. Galectins as modulators of tumor progression. Nat Rev Cancer 2005; 5:29–41.
5. Zhu C, Anderson AC, Schubart A, Xiong H, Imitola J, Khoury SJ, Zheng XX, Strom TB, Kuchroo VK. The Tim-3 ligand galectin-9 negatively regulates T helper type 1 immunity. Nat Immunol 2005; 6:1245–1252.
6. Kashio Y, Nakamura K, Abedin MJ, Seki M, Nishi N, Yoshida N, Nakamura T, Hirashima M. Galectin-9 induces apoptosis through the calcium-calpain-caspase-1 pathway. J Immunol 2003; 170:3631–3636.
7. Niwa H, Satoh T, Matsushima Y, Hosoya K, Saeki K, Niki T, Hirashima M, Yokozeki H. Stable form of galectin-9, a Tim-3 ligand, inhibits contact hypersensitivity and psoriatic reactions: a potent therapeutic tool for Th1- and/or Th17-mediated skin inflammation. Clin Immunol 2009; 132: 184–194.
8. Dai SY, Nakagawa R, Itoh A, Murakami H, Kashio Y, Abe H, Katoh S, Kontani K, Kihara M, Zhang SL, Hata T, Nakamura T, et al. Galectin-9 induces maturation of human monocyte-derived dendritic cells. J Immunol 2005; 175:2974–2981.
9. Wang F, He W, Yuan J, Wu K, Zhou H, Zhang W, Chen ZK. Activation of Tim-3-Galectin-9 pathway improves survival of fully allogeneic skin grafts. Transpl Immunol 2008; 19:12–19.
10. Seki M, Oomizu S, Sakata KM, Sakata A, Arikawa T, Watanabe K, Ito K, Takeshita K, Niki T, Saita N, Nishi N, Yamauchi A, et al. Galectin-9 suppresses the generation of Th17, promotes the induction of regulatory T cells, and regulates experimental autoimmune arthritis. Clin Immunol 2008; 127:78–88.
11. Blois SM, Ilarregui JM, Tometten M, Garcia M, Orsal AS, Cordo-Russo R, Toscano MA, Bianco GA, Kobelt P, Handjiski B, Tirado I, Markert

UR, et al. A pivotal role for galectin-1 in fetomaternal tolerance. Nat Med 2007; 13:1450–1457.
12. Popovici RM, Krause MS, Germeyer A, Strowitzki T, von Wolff M. Galectin-9: a new endometrial epithelial marker for the mid- and late-secretory and decidual phases in humans. J Clin Endocrinol Metab 2005; 90:6170–6176.
13. Shimizu Y, Kabir-Salmani M, Azadbakht M, Sugihara K, Sakai K, Iwashita M. Expression and localization of galectin-9 in the human uterodome. Endocr J 2008; 55:879–887.
14. Thijssen VL, Hulsmans S, Griffioen AW. The galectin profile of the endothelium: altered expression and localization in activated and tumor endothelial cells. Am J Pathol 2008; 172:545–553.
15. Froehlich R, Hambruch N, Haeger JD, Dilly M, Kaltner H, Gabius HJ, Pfarrer C. Galectin fingerprinting detects differences in expression profiles between bovine endometrium and placentomes as well as early and late gestational stages. Placenta 2012; 33:195–201.
16. Spitzenberger F, Graessler J, Schroeder HE. Molecular and functional characterization of galectin 9 mRNA isoforms in porcine and human cells and tissues. Biochimie 2001; 83:851–862.
17. Chabot S, Kashio Y, Seki M, Shirato Y, Nakamura K, Nishi N, Nakamura T, Matsumoto R, Hirashima M. Regulation of galectin-9 expression and release in Jurkat T cell line cells. Glycobiology 2002; 12:111–118.
18. Zhang F, Zheng M, Qu Y, Li J, Ji J, Feng B, Lu A, Wang M, Liu B. Different roles of galectin-9 isoforms in modulating E-selectin expression and adhesion function in LoVo colon carcinoma cells. Mol Biol Rep 2009; 36:823–830.
19. Clark DA, Banwatt D, Chaouat G. Stress-triggered abortion in mice prevented by alloimmunization. Am J Reprod Immunol 1993; 29: 141–147.
20. Clark DA, Arck PC, Chaouat G. Why did your mother reject you? Immunogenetic determinants of the response to environmental selective pressure expressed at the uterine level. Am J Reprod Immunol 1999; 41: 5–22.
21. Lin H, Mosmann TR, Guilbert L, Tuntipopipat S, Wegmann TG. Synthesis of T helper 2-type cytokines at the maternal-fetal interface. J Immunol 1993; 151:4562–4573.
22. Piccinni MP, Beloni L, Livi C, Maggi E, Scarselli G, Romagnani S. Defective production of both leukemia inhibitory factor and type 2 T-helper cytokines by decidual T cells in unexplained recurrent abortions. Nat Med 1998; 4:1020–1024.
23. Blois SM, Joachim R, Kandil J, Margni R, Tometten M, Klapp BF, Arck PC. Depletion of CD8+ cells abolishes the pregnancy protective effect of progesterone substitution with dydrogesterone in mice by altering the Th1/Th2 cytokine profile. J Immunol 2004; 172:5893–5899.
24. Clark DA, Yu G, Arck PC, Levy GA, Gorczynski RM. MD-1 is a critical part of the mechanism causing Th1-cytokine-triggered murine fetal loss syndrome. Am J Reprod Immunol 2003; 49:297–307.
25. Nishi N, Itoh A, Shoji H, Miyanaka H, Nakamura T. Galectin-8 and galectin-9 are novel substrates for thrombin. Glycobiology 2006; 16: 15C–20C.
26. Yamamoto H, Kashio Y, Shoji H, Shinonaga R, Yoshimura T, Nishi N, Nabe T, Nakamura T, Kohno S, Hirashima M. Involvement of galectin-9 in guinea pig allergic airway inflammation. Int Arch Allergy Immunol 2007; 143(suppl 1):95–105.
27. Li Y, Feng J, Geng S, Wei H, Chen G, Li X, Wang L, Wang R, Peng H, Han G, Shen B. The N- and C-terminal carbohydrate recognition domains of galectin-9 contribute differently to its multiple functions in innate immunity and adaptive immunity. Mol Immunol 2011; 48:670–677.
28. Dey SK, Lim H, Das SK, Reese J, Paria BC, Daikoku T, Wang H. Molecular cues to implantation. Endocr Rev 2004; 25:341–373.
29. Kadowaki T, Arikawa T, Shinonaga R, Oomizu S, Inagawa H, Soma G, Niki T, Hirashima M. Galectin-9 signaling prolongs survival in murine lung-cancer by inducing macrophages to differentiate into plasmacytoid dendritic cell-like macrophages. Clin Immunol 2012; 142:296–307.
30. Nobumoto A, Nagahara K, Oomizu S, Katoh S, Nishi N, Takeshita K, Niki T, Tominaga A, Yamauchi A, Hirashima M. Galectin-9 suppresses tumor metastasis by blocking adhesion to endothelium and extracellular matrices. Glycobiology 2008; 18:735–744.
31. Kageshita T, Kashio Y, Yamauchi A, Seki M, Abedin MJ, Nishi N, Shoji H, Nakamura T, Ono T, Hirashima M. Possible role of galectin-9 in cell aggregation and apoptosis of human melanoma cell lines and its clinical significance. Int J Cancer 2002; 99:809–816.
32. Yamauchi A, Kontani K, Kihara M, Nishi N, Yokomise H, Hirashima M. Galectin-9, a novel prognostic factor with antimetastatic potential in breast cancer. Breast J 2006; 12:S196–S200.
33. Dziadek M, Darling P, Zhang RZ, Pan TC, Tillet E, Timpl R, Chu ML. Expression of collagen alpha 1(VI), alpha 2(VI), and alpha 3(VI) chains in the pregnant mouse uterus. Biol Reprod 1995; 52:885–894.
34. Guimond MJ, Luross JA, Wang B, Terhorst C, Danial S, Croy BA. Absence of natural killer cells during murine pregnancy is associated with reproductive compromise in TgE26 mice. Biol Reprod 1997; 56:169–179.
35. Adamson SL, Lu Y, Whiteley KJ, Holmyard D, Hemberger M, Pfarrer C, Cross JC. Interactions between trophoblast cells and the maternal and fetal circulation in the mouse placenta. Dev Biol 2002; 250:358–373.
36. Zhang J, Chen Z, Smith GN, Croy BA. Natural killer cell-triggered vascular transformation: maternal care before birth? Cell Mol Immunol 2011; 8:1–11.
37. Girardi G, Yarilin D, Thurman JM, Holers VM, Salmon JE. Complement activation induces dysregulation of angiogenic factors and causes fetal rejection and growth restriction. J Exp Med 2006; 203:2165–2175.
38. Lipkowitz MS, Leal-Pinto E, Cohen BE, Abramson RG. Galectin 9 is the sugar-regulated urate transporter/channel UAT. Glycoconj J 2004; 19: 491–498.